Inorganic Chemistry

Article

pubs.acs.org/IC

Synthesis and Isomerization of N-Fused Tetraphenylporphyrin Ruthenium(II) Complexes

Motoki Toganoh,[†] Hideaki Matsuo,[†] Ayumi Sato,[†] Yuya Hirashima,[†] and Hiroyuki Furuta*[,†,‡]

[†]Department of Chemistry and Biochemistry, Graduate School of Engineering, Kyushu University, 744 Moto-oka, Nishi-ku, Fukuoka 819-0395, Japan

[‡]Center for Molecular Systems, Kyushu University, 744 Moto-oka, Nishi-ku, Fukuoka 819-0395, Japan

Supporting Information

ABSTRACT: Three possible isomers of N-fused tetraphenylporphyrin ruthenium complexes, Ru(NFTPp)Cl(CO)$_2$ (**2a−c**), were isolated and fully characterized by NMR, IR, CV, UV−vis-NIR absorption, and X-ray crystallographic analyses. Each isomer was stable at ambient conditions and isomerization among **2a−c** occurred at elevated temperature both in solution and in a solid state, through the intramolecular rotational pathways. Electronic structures of **2a−c** were analyzed in detail by DFT study to reveal appreciable differences in the interaction between the NFTPp ligand and the Ru−Cl moiety.

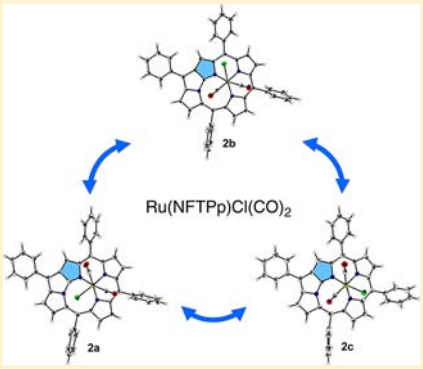

INTRODUCTION

A multidentate planar ligand offers a unique coordination environment on a metal center. For example, π-planar ligands, such as an η^5-cyclopentadienyl ligand and an η^6-benzene ligand, are widely used in transition metal complexes for targeting catalysts as well as functional molecules.[1,2] Generally, these ligands are freely rotating at room temperature on a center metal in solution and then the electronic effect imposed by the ligands to the center metal is dynamically averaged even when they have the less symmetrical structures like an indenyl ligand and a *p*-cymene ligand.[3] Aside from such π-ligands, we have been interested in a unique unsymmetrical multidentate planar ligand named N-fused porphyrinato (NFp),[4] which is a mononegative six-electron donating tridentate nitrogen ligand showing characteristic photophysical properties.[5] Three nitrogen atoms in the NFp ligand are arranged in a triangle manner to bind a metal ion tightly (Chart 1). Accordingly, no ligand rotation on the center metal is observed even at elevated temperature as illustrated by a ferrocene-type complex, Fe(NFp)$_2$, unlike the case of other porphyrinoids.[6] Successful isolation of a single isomer of Fe(NFp)$_2$ stimulated us to investigate an unsymmetrical nature of NFp metal complexes in detail. Isomerization process of counter ligands on the metal center would be also a subject of general interest.

Study on the transition metal complexes of NFp is a developing subject and the examples are still limited.[7] Previously, we reported the rhenium and manganese complexes bearing NFp ligand, Re(NFp)(CO)$_3$,[8] and Mn(NFp)(CO)$_3$.[9] Re(NFp)(CO)$_3$ was oxidized under mild oxidation conditions to afford Re(NFp)O$_3$,[10] which could serve as a catalyst in the oxygen atom transfer reactions.[11] Although these complexes showed interesting properties, they commonly have three identical ligands (carbonyl or oxo) other than NFp and an unsymmetrical nature of NFp ligand has not yet been studied. Additionally, unique transformations of NFp were reported by insertion of main group elements such as boron,[12] phosphorus,[13] and silicon.[14]

Chart 1. NFp Transition Metal Complexes

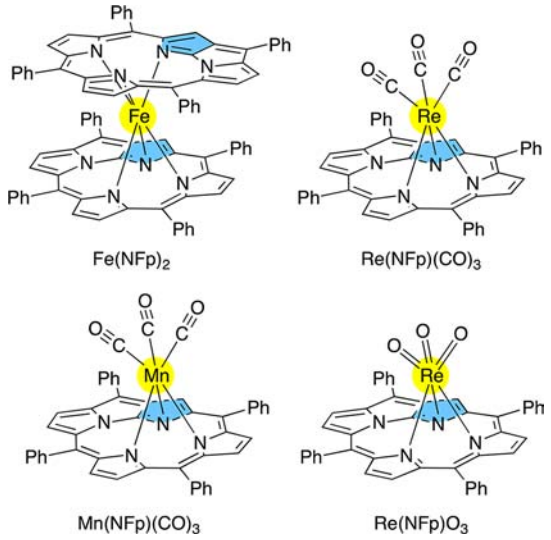

Received: May 31, 2013
Published: August 5, 2013

   dx.doi.org/10.1021/ic401314a | *Inorg. Chem.* 2013, 52, 9613−9619

Scheme 1. Synthesis of Ru(NFTPp)Cl(CO)$_2$ (2a−c)

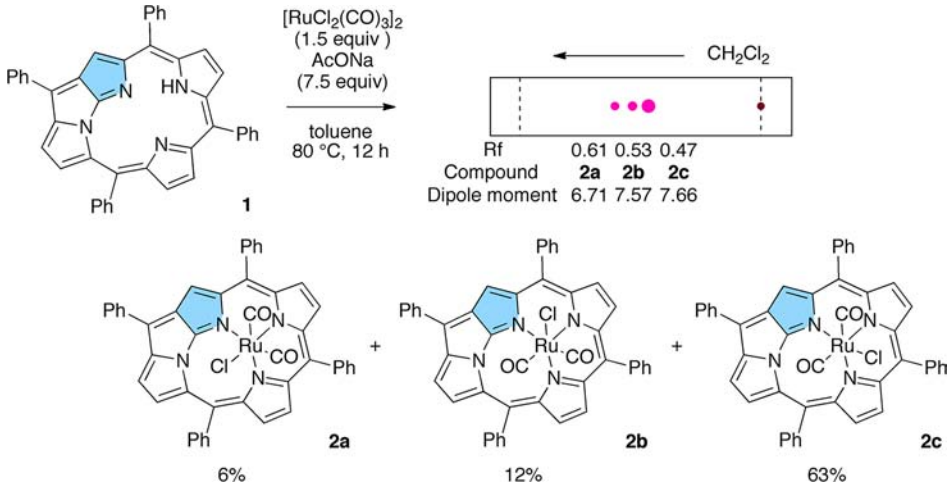

This time ruthenium complexes bearing a N-fused tetraphenylporphyrinato ligand, Ru(NFTPp)Cl(CO)$_2$, were prepared for the first time and possible three isomers were successfully isolated and characterized, which afforded various information on unsymmetrical multidentate planar ligands.

EXPERIMENTAL SECTION

General. All of the reactions were performed in oven-dried reaction vessels under Ar or N_2. Commercially available solvents and reagents were used without further purification unless otherwise mentioned. CH_2Cl_2 was dried by passing through a pad of alumina. Toluene was distilled over CaH_2. Thin-layer chromatography (TLC) was carried out on aluminum sheets coated with silica gel 60 F_{254} (Merck). Preparative separation was performed by silica gel flash column chromatography (KANTO Silica Gel 60 N, spherical, neutral, 40−50 μm) or silica gel gravity column chromatography (KANTO Silica Gel 60 N, spherical, neutral, 63−210 μm). ^{1}H NMR spectra were recorded in $CDCl_3$ solution on a JNM-AL SERIES FT-NMR spectrometer (JEOL) at 300 MHz, and chemical shifts were reported relative to a residual proton of a deuterated solvent, $CHCl_3$ (δ = 7.26) in ppm. ^{13}C NMR spectra were recorded in $CDCl_3$ solution on the same instrument at 75 MHz, and chemical shifts were reported relative to $CDCl_3$ (δ = 77.00) in ppm. UV−vis-NIR absorption spectra were recorded on a UV-3150PC spectrometer (Shimadzu) with a photomultiplier tube detector (190−750 nm) and a PbS detector (750−3200 nm). Mass spectra were recorded on an autoflex MALDI−TOF MS spectrometer (Bruker Daltonics). For elemental analyses, samples were recrystallized from CH_2Cl_2 and dried under reduced pressure at ambient temperature except for **2b**. Since complete removal of CH_2Cl_2 from samples without decomposition was difficult, samples containing CH_2Cl_2 were used for elemental analyses. Cyclic voltammetric measurements were performed on a CH Instrument Model 620B (ALS) equipped with a Pt electrode. All of the measurements were achieved in 0.1 M Bu_4NPF_6 solution of CH_2Cl_2 (deoxygenated by Ar bubbling over 30 min) with the scan rate of 100 mV/s under Ar atmosphere. A Ag/Ag+ electrode was used for the reference electrode and freshly sublimed ferrocene was used as external standard to determine redox potentials. IR absorptions were recorded on an FT/IR-4200 (JASCO).

Preparation of 2a−c. A mixture of **1** (30.0 mg, 0.049 mmol), $[RuCl_2(CO)_3]_2$ (19.2 mg, 0.037 mmol), and CH_3COONa (30.8 mg, 0.38 mmol) in 15 mL of toluene was heated at 80 °C for 12 h under Ar. After evaporation, the residue was separated by silica gel column chromatography with CH_2Cl_2/hexane = 3/1 (v/v) to give **2a** (2.3 mg, 2.9 μmol, 6% yield), **2b** (4.7 mg, 5.8 μmol, 12% yield), and **2c** (24.9 mg, 31.0 μmol, 63% yield).

2a: ^{1}H NMR ($CDCl_3$, 300 MHz, ppm): δ 7.11 (d, J = 4.5 Hz, 1H), 7.36 (d, J = 4.8 Hz, 1H), 7.57 (t, J = 7.8 Hz, 1H), 7.61−7.85 (m, 16H), 7.90 (d, J = 4.8 Hz, 1H), 8.12−8.16 (m, 2H), 8.66 (d, J = 7.8 Hz, 2H), 8.74 (d, J = 5.2 Hz, 1H), 9.18 (d, J = 5.2 Hz, 1H), 9.37 (s, 1H); ^{13}C NMR ($CDCl_3$, 75 MHz, ppm): δ 112.51, 120.99, 123.11, 123.39, 125.96, 127.66, 128.12, 128.35, 128.62, 129.50, 129.57, 129.81, 132.13, 133.06, 133.28, 134.48, 134.80, 137.02, 137.21, 137.45, 137.96, 139.72, 144.21, 144.90, 149.60, 152.30, 152.49, 154.73, 157.60, 161.05, 192.18, 192.44; IR (powder, cm^{-1}): 2042 (CO), 1978 (CO); Anal. Calcd for **2a**·0.6CH_2Cl_2: C, 65.45; H, 3.32; N, 6.55. Found: C, 65.48; H, 3.26; N, 6.65; MS (LDI, positive): m/z = 747.85 [M−2(CO)]$^+$, 712.81 [M−2(CO)−Cl]$^+$; UV−vis-NIR (CH_2Cl_2, λ_{max}/nm (log ε)): 963 (3.60), 873 (3.58), 653 (3.80), 522 (4.75), 450 (4.42), 354 (4.68).

2b: ^{1}H NMR ($CDCl_3$, 300 MHz, ppm): δ 7.17 (d, J = 4.8 Hz, 1H), 7.34 (d, J = 4.5 Hz, 1H), 7.52−7.56 (m, 2H), 7.61−7.65 (m, 4H), 7.71−7.83 (m, 10H), 7.95−7.99 (m, 2H), 8.21−8.25 (m, 2H), 8.62−8.67 (m, 3H), 9.18 (d, J = 5.1 Hz, 1H), 9.29 (s, 1H); ^{13}C NMR ($CDCl_3$, 75 MHz, ppm): δ 113.31, 114.68, 118.36, 121.84, 125.31, 127.08, 127.66, 127.76, 127.95, 128.39, 128.54, 128.64, 129.01, 129.39, 129.83, 131.24, 131.27, 132.39, 132.56, 134.63, 136.18, 137.34, 137.74, 138.24, 141.42, 143.08, 144.57, 147.06, 152.06, 152.32, 152.95, 158.27, 163.47, 192.19, 192.71; IR (powder, cm^{-1}): 2042 (CO), 1978 (CO); Anal. Calcd for **2b**·2CH_2Cl_2: C, 59.18; H, 3.21; N, 5.75. Found: C, 59.23; H, 3.29; N, 5.84; MS (LDI, positive): m/z = 747.92 [M−2(CO)]$^+$, 712.92 [M−2(CO)−Cl]$^+$; UV−vis-NIR (CH_2Cl_2, λ_{max}/nm (log ε)): 950 (3.49), 861 (3.53), 646 (sh) (3.62), 522 (4.73), 421 (sh) (4.33), 360 (4.60).

2c: ^{1}H NMR ($CDCl_3$, 300 MHz, ppm): δ 7.39 (d, J = 4.5 Hz, 1H), 7.45 (d, J = 4.8 Hz, 1H), 7.52−7.64 (m, 5H), 7.72−7.80 (m, 5H), 7.82−7.87 (m, 4H), 7.96−8.02 (m, 2H), 8.05−8.09 (m, 2H), 8.16−8.20 (m, 2H), 8.68 (d, J = 7.2 Hz, 2H), 8.86 (d, J = 5.2 Hz, 1H), 9.27 (d, J = 5.2 Hz, 1H), 9.35 (s, 1H); ^{13}C NMR ($CDCl_3$, 75 MHz, ppm): δ 111.93, 112.22, 119.15, 121.49, 125.30, 126.76, 127.41, 127.60, 127.94, 128.40, 128.44, 128.52, 128.65, 129.38, 129.59, 129.89, 130.30, 130.44, 132.02, 132.77, 133.35, 134.63, 136.30, 137.26, 138.09, 139.04, 139.60, 142.13, 144.52, 148.47, 151.86, 153.04, 157.34, 163.41, 191.89, 192.15; IR (powder, cm^{-1}): 2034 (CO), 1972 (CO); Anal. Calcd for **2c**·0.3CH_2Cl_2: C, 67.02; H, 3.35; N, 6.75. Found: C, 66.84; H, 3.34; N, 6.78; MS (LDI, positive): m/z = 748.11 [M−2(CO)]$^+$, 712.90 [M−2(CO)−Cl]$^+$; UV−vis-NIR (CH_2Cl_2, λ_{max}/nm (log ε)): 939 (3.44), 849 (3.45), 646 (3.65), 513 (4.77), 418 (4.40), 352 (4.62).

X-ray Crystallography. X-ray analysis of **2a** was performed on a Saturn equipped with a CCD detector (RIGAKU) using MoKα (graphite, monochromated, λ = 0.710747 Å) radiation. X-ray analyses of **2b** and **2c** were performed on a SMART APEX equipped with a CCD detector (Bruker) using MoKα (graphite, monochromated, λ = 0.71069 Å) radiation. The structure was solved by the direct method of SHELXS-97 and refined using the SHELXL-97 program.[15] All of the positional parameters and thermal parameters of non-hydrogen atoms were refined anisotropically on F^2 by the full-matrix least-

dx.doi.org/10.1021/ic401314a | Inorg. Chem. 2013, 52, 9613−9619

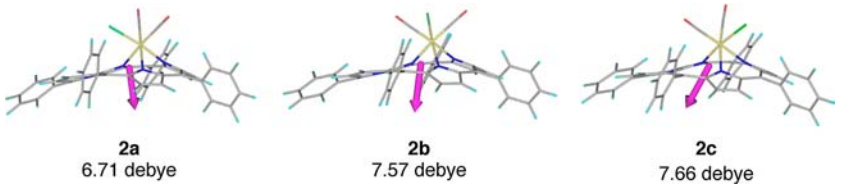

Figure 1. DFT calculated dipole moments for **2a**−**c**.

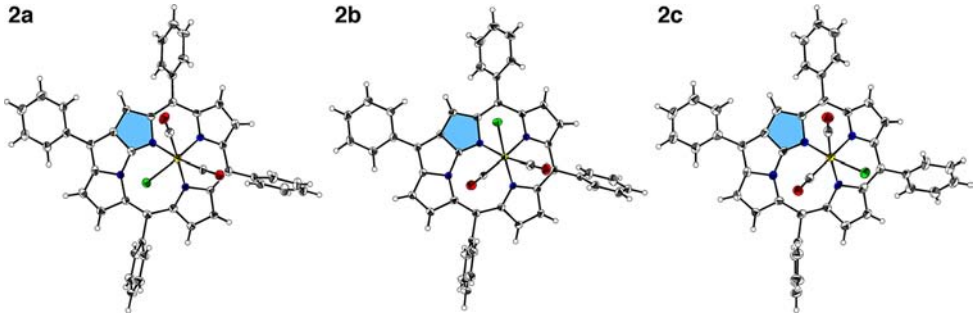

Figure 2. X-ray structures of **2a**−**c**. The thermal ellipsoids are described at the 30% probability level.

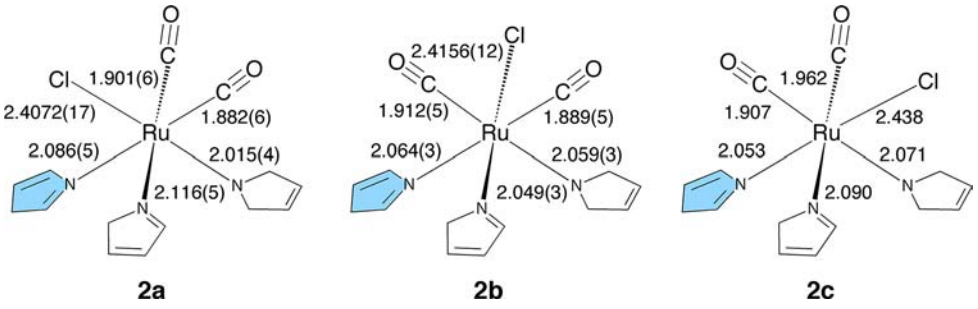

Figure 3. Selected bond lengths in Å around the metal centers in **2a**−**c**. Averaged values of two independent molecules are shown in **2c**.

squares method. Hydrogen atoms were placed at the calculated positions and refined riding on their corresponding carbon atoms.

Calculation Details. All density functional theory calculations were achieved with a Gaussian09 program package.[16] The basis sets implemented in the program were used. The B3LYP density functional method was used with a 631LAN basis set for structural optimizations and frequency calculation.[17] The 631LAN bases set is composed of 6-31G** for carbon, hydrogen, nitrogen, oxygen, and chloride and LANL2DZ for ruthenium. Initial structures for ground state were based on the X-ray structures and those for transition state were arbitrarily constructed. Ground state geometries were fully optimized and verified by the frequency calculations, where no imaginary frequency was found. Transition state geometries were also verified by the frequency calculations, where only one imaginary frequency was found. Vibrational modes corresponding to imaginary frequency were consistent with the rotational mechanism discussed below.

RESULTS AND DISCUSSION

Upon heating of N-fused tetraphenylporphyrin (NFTPpH, **1**) with $[RuCl_2(CO)_3]_2$ and AcONa in toluene at reflux,[18] three spots were detected by the TLC analysis on the crude product (Scheme 1). Isolation of each compound can be achieved by standard silica gel column chromatography to afford three isomers of $Ru(NFTPp)Cl(CO)_2$ in 6% (**2a**), 12% (**2b**), and 63% (**2c**) yields, respectively (81% total yield). The ruthenium complexes **2a**−**c** were thermally stable both in solution and in a solid state until 120 °C, in which no isomerization among **2a**−**c** was observed. In addition, no isomerization was observed during standard purification manipulation. In the laser desorption/ionization (LDI) mass spectra, the reasonable fragment peaks assignable to $[M-2(CO)]^+$ and $[M-2(CO)-Cl]^+$ were observed for **2a**−**c**. In the ^1H NMR spectra, similar but different signals were observed for each complex. For example, singlet signals due to β-pyrrolic CH proton of N-confused pyrrole ring, which was shaded in blue in Scheme 1 at the tripentacyclic moiety, appeared at δ 9.37 (**2a**), 9.29 (**2b**), and 9.35 (**2c**) ppm, respectively. The signals due to the CO ligands were clearly observed in the ^{13}C NMR spectra at δ 192.18, 192.44 (**2a**), 192.19, 192.71 (**2b**), and 191.89, 192.15 (**2c**) ppm. Observation of the other ^1H and ^{13}C NMR signals in standard aromatic regions suggests their diamagnetic character. Presence of the CO ligands was also confirmed by the IR spectra, where the strong absorptions corresponding to the CO stretching were observed at 2042, 1978 (**2a**), 2046, 1985 (**2b**), and 2034, 1972 (**2c**) cm^{-1}, respectively. These values are comparable to the corresponding cyclopentadienyl ruthenium complex.[19]

Interestingly, the relative Rf values of $Ru(NFTPp)Cl(CO)_2$ would be predictable from the theoretical dipole moment. The dipole moments of **2a**−**c** calculated by a DFT method are shown in Figure 1. Basically, all of the dipole moments point from the metal center to the NFp plane, but slightly incline against the chloride ligand. The order of the magnitude of dipole moments in debye [**2a** (6.71) < **2b** (7.57) < **2c** (7.66)] is in good agreement with that of the Rf values [**2a** (0.61) > **2b** (0.53) > **2c** (0.47)]. Thus, simple TLC analysis might be

dx.doi.org/10.1021/ic401314a | Inorg. Chem. 2013, 52, 9613−9619

Table 1. Crystal Data and Structure Analysis Results for 2a−c

	2a	2b·CH_2Cl_2	2c
formula	$C_{46}H_{27}ClN_4O_2Ru$	$C_{47}H_{29}Cl_3N_4O_2Ru$	$2(C_{46}H_{27}ClN_4O_2Ru)$
cryst syst	monoclinic	triclinic	monoclinic
space group	$P2_1/n$	$P\bar{1}$	$P2_1/n$
R	0.0742	0.0513	0.0982
w$R2$ (all data)	0.2115	0.1248	0.2889
GOF	1.022	0.941	1.046
a (Å)	14.818(8)	9.7741(7)	10.102(5)
b (Å)	12.632(6)	12.5610(9)	24.532(13)
c (Å)	20.895(11)	16.6774(13)	30.099(15)
α (deg)	90	103.6270(10)	90
β (deg)	103.401(6)	94.340(2)	91.941(5)
γ (deg)	90	103.108(2)	90
V (Å^3)	3805(3)	1919.9(2)	7455(7)
Z	4	2	4
T (K)	123	173	223
cryst size (mm^3)	0.27 × 0.05 × 0.05	0.18 × 0.11 × 0.04	0.23 × 0.02 × 0.02
D_{calcd} (g cm^{-3})	1.404	1.538	1.433
$2\theta_{min}$, $2\theta_{max}$(deg)	3.8, 52.0	3.4, 52.0	4.3, 51.0
no. of rflns measd (unique)	7447	7497	13753
no. of rflns measd ($I > 2\sigma(I)$)	4905	5216	8456
no. of params	487	514	974
Δ (e Å^{-3})	1.149, −1.609	1.611, −0.683	2.923, −1.119
CCDC number	941077	941078	941079

effective to predict isomeric structures in metal complexes bearing unsymmetrical planar ligands.

The structures of **2a−c** were unambiguously determined by X-ray crystallographic analyses (Figure 2). Obviously, **2a−c** are isomers of $Ru(NFTPp)Cl(CO)_2$, which demonstrates the absence of NFp ligand rotation under the ambient conditions. In all of the complexes, the ruthenium metal is coordinated by two carbonyl ligands (neutral) and one chloride ligand (mononegative) in addition to the three nitrogen atoms of NFTPp ligand (mononegative in total). Accordingly, formal charge on the ruthenium center is +2 (d^6), which is consistent with the diamagnetic character. The complexes **2a−c** satisfy the 18-electron rule and take the distorted octahedral molecular geometry. The bond lengths around the metal centers are summarized in Figure 3. In spite of their similar molecular shapes, single crystals obtained so far showed the different unit cell in **2a−c** (Table 1). Single crystals of the same unit cell were not yet obtained even by recrystallization from the same solvents. Accordingly, comparison of bond lengths among **2a−c** would demand some caution. Nevertheless, we can recognize some sign of unsymmetrical nature in the NFp ligand. Possibly due to the trans effect imposed by the N-confused pyrrole moiety (colored pyrrole), the Ru−Cl bond length in **2c** (2.438 Å) is slightly longer than those in **2a** (2.407 Å) and **2b** (2.416 Å). In contrast, the Ru−CO bond lengths trans to the N-confused pyrrole in **2a** (1.882 Å) and **2b** (1.889 Å) are slightly shorter than the other Ru−CO bond lengths (av 1.921 Å). This might mean that electron donation from the N-confused pyrrole to the metal center would be stronger than those from the other regular pyrroles though all the pyrrole rings are fully conjugated to form an [18]annulenic π-circuit. Nevertheless, these bond lengths are roughly comparable to the corresponding cyclopentadienyl complexes.[20]

While no isomerization among **2a−c** was observed at 120 °C in toluene or chlorobenzene without additives, it occurred at higher temperature or in the presence of ruthenium reagent. As described above, when the reaction was performed at relatively low temperature like 80 °C, **2c** was obtained as the major product (**2a**:**2b**:**2c** = 7:15:78, based on the isolated amounts). Theoretically, **2c** is more stable than **2a** and **2b** only by 0.15 and 0.12 kcal/mol, respectively. Thus the product ratio at 80 °C would be under kinetic control.[21] When isolated pure **2c** was heated at 150 °C for 3.5 days in 1,2-dichlorobenzene under N_2, a mixture of **2a−c** was obtained in a ratio of 27:33:40 (**2a**:**2b**:**2c**), which clearly showed that the isomerization among **2a−c** occurred at elevated temperature. The ratio after isomerization was determined by the ^1H NMR analysis on the crude product. No distinct decomposition was observed during this isomerization, which was checked by TLC as well as ^1H NMR analyses. Interestingly, the isomerization was also observed in a solid state.[22] When **2c** (powder) was heated in a sealed tube at 180 °C for 50 h, a mixture of **2a−c** was obtained in a ratio of 12:24:64 (**2a**:**2b**:**2c**). In addition, the effect of additives for isomerization was examined. Although $Bu_4N^+Cl^-$ did not facilitate the isomerization, ruthenium reagent effectively affected the isomerization process. For example, upon heating of **2c** in toluene at 100 °C for 20 h in the presence of $[RuCl_2(CO)_3]_2$, a mixture of **2a−c** was obtained in a ratio of 18:32:50 (**2a**:**2b**:**2c**). Accordingly, the product ratio in the preparation of **2a−c** is somewhat unreproducible. Although the role of ruthenium reagent was yet unclear, temporary formation of binuclear ruthenium μ-Cl or μ-CO complexes might facilitate the isomerization process.[23]

Since the tridentate NFp ligand would tightly bind the ruthenium metal, the isomerization process should occur only with the rest three ligands, namely, one chloride and two carbonyl ligands. Besides, the isomerization should proceed intramolecularly because it occurred without any additives in a diluted solution or even in a solid state. Briefly, ligand dissociation/association would not occur during isomerization.[24] On the basis of the previous studies on intramolecular ligand exchange reactions of hexacoordinate octahedral

dx.doi.org/10.1021/ic401314a | Inorg. Chem. 2013, 52, 9613−9619

Scheme 2. Intramolecular Ligand Rearrangement in Hexacoordinate Octahedral NFp Complexes

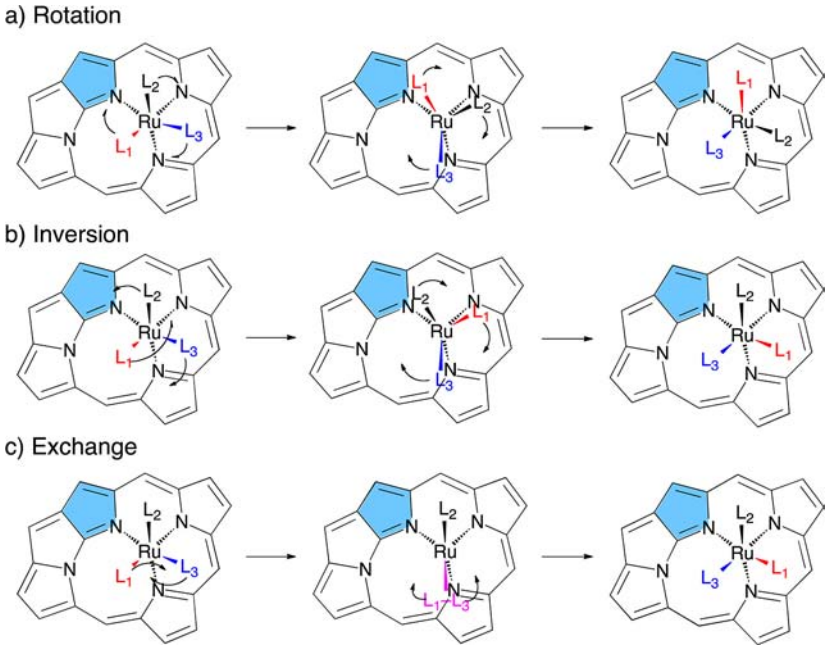

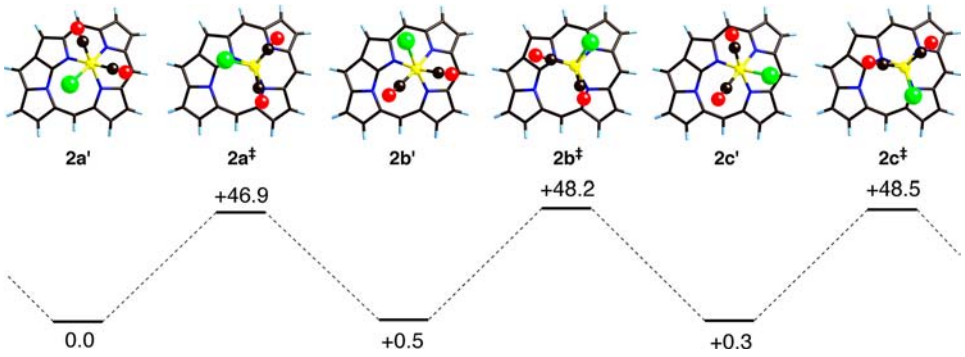

Figure 4. Energy profile for the rotation pathway in kcal/mol.

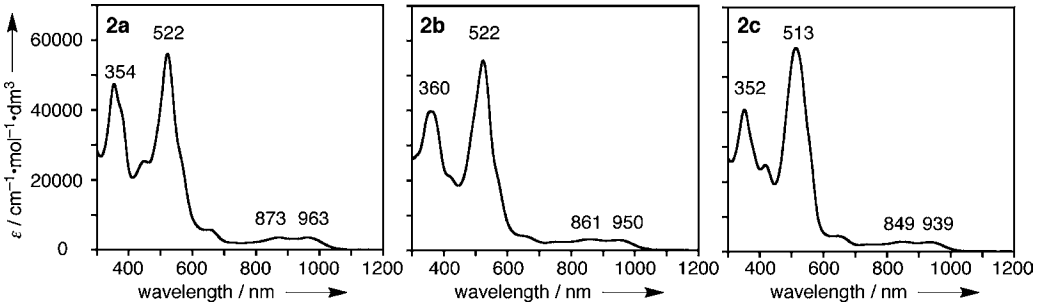

Figure 5. Absorption spectra of **2a–c** in CH_2Cl_2.

complexes, three pathways are postulated (Scheme 2).[25] A rotation pathway (a) is commonly proposed for intramolecular ligand exchange in the hexacoordinate octahedral complexes and would be most likely mechanism in this case.[26] Rotation should occur in a clockwise direction or counterclockwise direction, but only the former is shown in the scheme. An inversion pathway (b) is somewhat similar to pseudorotation of pentacoordinate complexes, which requires overall rearrangement of six ligands.[27] Thus it should not be probable with the rigid planar tridentate ligand. An exchange pathway (c) is sometimes suggested also, but it usually requires association/dissociation between two ligands, which is not expected in this case, namely between carbonyl and chloride ligands.[28] Accordingly, only the rotation pathway would be reasonable for hexacoordinate NFp complexes. To check the validity of the rotation pathway, an energy profile for meso-unsubstituted NFp ruthenium complexes was calculated by DFT methods (Figure 4). Estimated activation energy is 46–49 kcal/mol, which would be appropriate values for thermal isomerization at 150–180 °C.[29]

The absorption spectra of **2a–c** in CH_2Cl_2 are shown in Figure 5. Basically, the absorption spectra of **2a–c** resemble

dx.doi.org/10.1021/ic401314a | Inorg. Chem. 2013, 52, 9613–9619

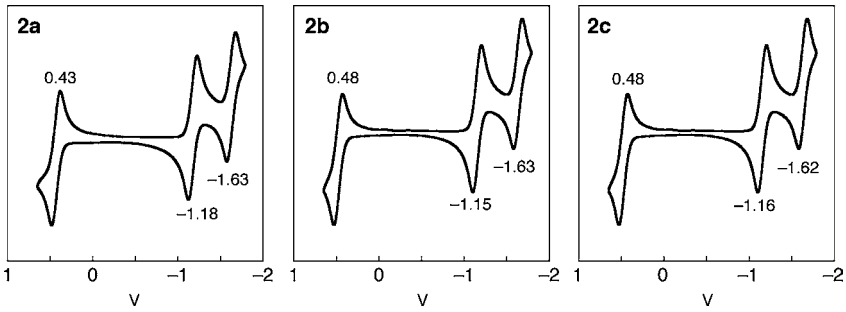

Figure 6. Cyclic voltammograms of **2a**−**c** in CH_2Cl_2 with 0.1 M Bu_4NPF_6 (Pt electrode, scan rate 100 mV/s, vs. Fc/Fc^+). The values indicate half-wave potentials in V.

that of the ligand **1**. For example, the Soret-like bands for **2a**−**c** appear at 522, 522, and 513 nm, respectively. Q-type bands are observed in the near-IR legion of 850−960 nm. Among three isomers, **2c** (939 nm) showed the small blue shift compared to **2a** (963 nm) and **2b** (950 nm). In the previous studies, the electron withdrawing groups at the N-confused pyrrole ring caused blue shifts in the Q-type bands region.[5] Thus the blue shift in **2c** might be explained by the electron withdrawing effect of the chloride ligand trans to the N-confused pyrrole ring.

The ruthenium complexes **2a**−**c** showed one reversible oxidation wave and two reversible reduction waves, similar to the reported NFp metal complexes (Figure 6).[8−10] Although no significant differences were observed in the half-wave potentials, **2a** shows the narrowest electrochemical HOMO−LUMO gap among three isomers (**2a**: 1.61 eV, **2b**: 1.63 eV, **2c**: 1.64 eV), which are in good agreement with its longest absorption maxima (**2a**: 963 nm, **2b**: 950 nm, **2c**: 939 nm).

Theoretical study on the electronic state of **2a**−**c** revealed distinct differences among them, which were consistent with the experimental observation. Figure 7 displays the HOMOs and LUMOs of **2a**−**c** and Figure 8 shows their orbital energies. The LUMOs of **2a**−**c** are quite similar to that of N-fused

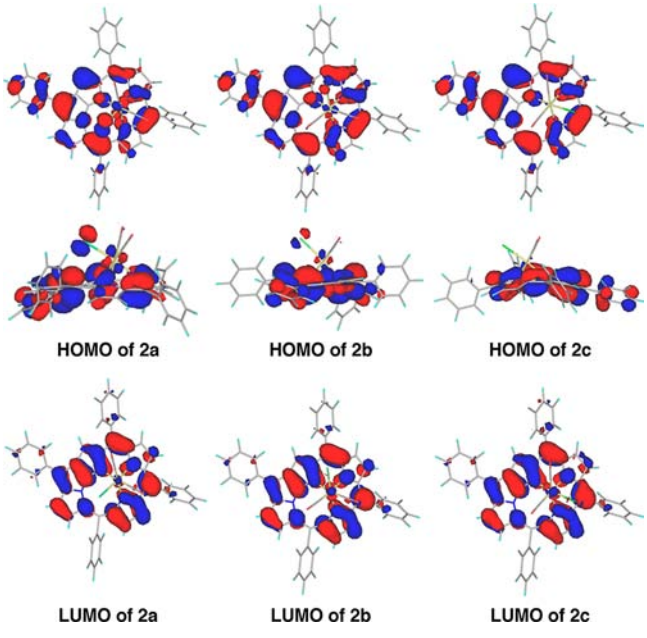

Figure 7. Kohn−Sham orbitals of **2a**−**c**. Top and side views are shown for HOMOs and top views are shown for LUMOs.

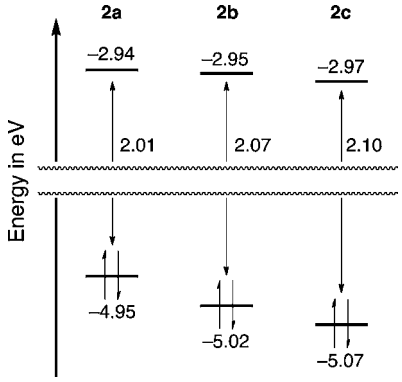

Figure 8. Theoretical orbital energies for HOMOs and LUMOs of **2a**−**c**.

porphyrin ligand except for small contribution of metal d orbital. No marked difference is observed among **2a**−**c**. Thus, the LUMO energies are insensitive to the structures (**2a**: −2.94 eV, **2b**: −2.95 eV, **2c**: −2.97 eV). In contrast, an appreciable difference is observed in the HOMOs of **2a**−**c**. There exists large contribution of Ru−Cl antibonding orbital in **2a** and moderate contribution in **2b**, while no contribution is observed in **2c**. Accordingly, **2a** has the highest HOMO energy (−4.95 eV), **2b** has the intermediary HOMO energy (−5.02 eV), and **2c** has the lowest HOMO energy (−5.07 eV). As a result, **2a** shows the narrowest HOMO−LUMO band gap of 2.01 eV, which is in good agreement with the CV and UV−vis-NIR results. Also, the HOMO−LUMO band gaps of **2b** (2.07 eV) and **2c** (2.10 eV) are corresponding to the experimental results. The contribution of Ru−Cl antibonding orbital in HOMOs would affect the atomic charge of chloride ligand also. The atomic polar tensor (APT) charge of chloride atom in **2a** (−0.39) is appreciably less negative than those in **2b** (−0.43) and **2c** (−0.46) in spite of the similar structures. This might mean that the position of chloride ligand in **2a** would be favorable for electron donation to the metal center. Actually, **2a** showed the shortest Ru−Cl bond length among **2a**−**c** in the X-ray structures.

■ CONCLUSIONS

In summary, three isomers of N-fused tetraphenylporphyrin ruthenium complexes, $Ru(NFTPp)Cl(CO)_2$ (**2a**−**c**), were isolated and fully characterized by NMR, IR, CV, NIR-UV−vis absorption, and X-ray crystallographic analyses. Appreciable differences in absorption wavelengths as well as electrochemical potentials among **2a**−**c** were observed, which would be explained by the relative positions of N-confused pyrrole ring

dx.doi.org/10.1021/ic401314a | Inorg. Chem. 2013, 52, 9613−9619

and chloride ligand or the interaction between NFp π-orbital and Ru−Cl σ^*-orbital. Upon heating, isomerization among **2a−c** was observed both in solution and in a solid state, which would proceed intramolecularly through the rotational pathway. Further studies on NFp metal complexes are now ongoing.

■ ASSOCIATED CONTENT

Supporting Information

^{1}H and ^{13}C NMR spectra of **2a−c**. Cartesian coordinates and vibrational frequencies for the optimized structures. This material is available free of charge via the Internet at http://pubs.acs.org.

■ AUTHOR INFORMATION

Corresponding Author

*E-mail: hfuruta@cstf.kyushu-u.ac.jp.

Notes

The authors declare no competing financial interest.

■ ACKNOWLEDGMENTS

The present work was supported by the Grant-in-Aid for Young Scientists (25870504) to M.T. and on Innovative Areas (231087015) to H.F. from the Ministry of Education, Culture, Sports, Science, and Technology of Japan.

■ REFERENCES

(1) (a) Field, L. D.; Lindall, C. M.; Masters, A. F.; Clentsmith, G. K. B. *Coord. Chem. Rev.* **2011**, *255*, 1733−1790. (b) Jutzi, P.; Buford, N. *Chem. Rev.* **1999**, *99*, 969−990. (c) Coville, N. J.; du Plooy, K. E.; Pickl, W. *Coord. Chem. Rev.* **1992**, *116*, 1−267.

(2) (a) Pampaloni, G. *Coord. Chem. Rev.* **2010**, *254*, 402−419. (b) Schmidbaur, H.; Schier, A. *Organometallics* **2008**, *27*, 2361−2395.

(3) (a) Peacock, A. F. A.; Habtemariam, A.; Fernández, R.; Walland, V.; Fabbiani, F. P. A.; Parsons, S.; Aird, R. E.; Jodrell, D. I.; Sadler, P. J. *J. Am. Chem. Soc.* **2006**, *128*, 1739−1748. (b) Chen, S.; Carperos, V.; Noll, B.; Swope, R. J.; DuBois, M. R. *Organometallics* **1995**, *14*, 1221−1231. (c) Sridevi, V. S.; Leong, W. K. *J. Organomet. Chem.* **2007**, *692*, 4909−4916.

(4) (a) Furuta, H.; Ishizuka, T.; Osuka, A.; Ogawa, T. *J. Am. Chem. Soc.* **1999**, *121*, 2945−2946. (b) Furuta, H.; Ishizuka, T.; Osuka, A.; Ogawa, T. *J. Am. Chem. Soc.* **2000**, *122*, 5748−5757. (c) Ishizuka, T.; Ikeda, S.; Toganoh, M.; Yoshida, I.; Ishikawa, Y.; Osuka, A.; Furuta, H. *Tetrahedron* **2008**, *64*, 4037−4050. (d) Touden, S.; Ikawa, Y.; Sakashita, R.; Toganoh, M.; Mori, S.; Furuta, H. *Tetrahedron Lett.* **2012**, *53*, 6071−6074.

(5) (a) Lee, J. S.; Lim, J. M.; Toganoh, M.; Furuta, H.; Kim, D. *Chem. Commun.* **2010**, *46*, 285−287. (b) Ikeda, S.; Toganoh, M.; Easwaramoorthi, S.; Lim, J. M.; Kim, D.; Furuta, H. *J. Org. Chem.* **2010**, *75*, 8637−8649.

(6) (a) Toganoh, M.; Sato, A.; Furuta, H. *Angew. Chem., Int. Ed.* **2011**, *50*, 2752−2755. (b) Berlicka, A.; Latos-Grażyński, L. *Inorg. Chem.* **2009**, *48*, 7922−7930.

(7) Toganoh, M.; Furuta, H. *Handbook of Porphyrin Science*; Kadish, K. M., Smith, K. M., Guilard, R., Eds.; World Scientific: Singapore, 2010; Vol. *2*, pp 295−367.

(8) (a) Toganoh, M.; Ishizuka, T.; Furuta, H. *Chem. Commun.* **2004**, 2464−2465. (b) Toganoh, M.; Ikeda, S.; Furuta, H. *Inorg. Chem.* **2007**, *46*, 10003−10015.

(9) Ikeda, S.; Toganoh, M.; Furuta, H. *Inorg. Chem.* **2011**, *50*, 6029−6043.

(10) Toganoh, M.; Ikeda, S.; Furuta, H. *Chem. Commun.* **2005**, 4589−4591.

(11) (a) Toganoh, M.; Fujino, K.; Ikeda, S.; Furuta, H. *Tetrahedron Lett.* **2008**, *49*, 1488−1491. (b) Toganoh, M.; Hihara, T.; Yonekura, K.; Ishikawa, Y.; Furuta, H. *J. Porphyrins Phthalocyanines* **2009**, *13*, 215−222.

(12) Młodzianowska, A.; Latos-Grażyński, L.; Szterenberg, L.; Stępień, M. *Inorg. Chem.* **2007**, *46*, 6950−6957.

(13) Młodzianowska, A.; Latos-Grażyński, L.; Szterenberg, L. *Inorg. Chem.* **2008**, *47*, 6364−6374.

(14) Skonieczny, J.; Latos-Grażyński, L.; Szterenberg, L. *Inorg. Chem.* **2009**, *48*, 7394−7407.

(15) Sheldrick, G. M. *Program for the Solution of Crystal Structures*; University of Göttingen: Göttingen, Germany, 1997.

(16) Frisch, M. J.; Trucks, G. W.; Schlegel, H. B.; Scuseria, G. E.; Robb, M. A.; Cheeseman, J. R.; Scalmani, G.; Barone, V.; Mennucci, B.; Petersson, G. A.; Nakatsuji, H.; Caricato, M.; Li, X.; Hratchian, H. P.; Izmaylov, A. F.; Bloino, J.; Zheng, G.; Sonnenberg, J. L.; Hada, M.; Ehara, M.; Toyota, K.; Fukuda, R.; Hasegawa, J.; Ishida, M.; Nakajima, T.; Honda, Y.; Kitao, O.; Nakai, H.; Vreven, T.; Montgomery, Jr., J. A.; Peralta, J. E.; Ogliaro, F.; Bearpark, M.; Heyd, J. J.; Brothers, E.; Kudin, K. N.; Staroverov, V. N.; Kobayashi, R.; Normand, J.; Raghavachari, K.; Rendell, A.; Burant, J. C.; Iyengar, S. S.; Tomasi, J.; Cossi, M.; Rega, N.; Millam, J. M.; Klene, M.; Knox, J. E.; Cross, J. B.; Bakken, V.; Adamo, C.; Jaramillo, J.; Gomperts, R.; Stratmann, R. E.; Yazyev, O.; Austin, A. J.; Cammi, R.; Pomelli, C.; Ochterski, J. W.; Martin, R. L.; Morokuma, K.; Zakrzewski, V. G.; Voth, G. A.; Salvador, P.; Dannenberg, J. J.; Dapprich, S.; Daniels, A. D.; Farkas, Ö.; Foresman, J. B.; Ortiz, J. V.; Cioslowski, J.; Fox, D. J. *Gaussian 09, Revision C.01*; Gaussian, Inc.: Wallingford CT, 2009.

(17) (a) Becke, A. D. *J. Phys. Chem.* **1993**, *98*, 5648−5652. (b) Lee, C.; Yang, W.; Parr, R. G. *Phys. Rev. B* **1988**, *37*, 785−789. (c) Vosko, S. H.; Wilk, L.; Nusair, M. *Can. J. Phys.* **1980**, *58*, 1200−1211. (d) Stephens, P. J.; Devlin, F. J.; Chabalowski, C. F.; Frisch, M. J. *J. Phys. Chem.* **1994**, *98*, 11623−11627.

(18) Bruce, M. I.; Sharrocks, D. N.; Stone, F. G. A. *J. Organomet. Chem.* **1971**, *31*, 269−273.

(19) Dev, S.; Selegue, J. P. *J. Organomet. Chem.* **1994**, *469*, 107−110.

(20) Fuller, R. O.; Griffith, C. S.; Koutsantonis, G. A.; Lapere, K. M.; Skelton, B. W.; Spackman, M. A.; White, A. H.; Wild, D. A. *CrystEngComm* **2012**, *14*, 812−818.

(21) The product ratio is roughly estimated to be 30:32:38 (**2a**:**2b**:**2c**) under thermodynamic control.

(22) (a) Coville, N. J.; Levendis, D. C. *Eur. J. Inorg. Chem.* **2002**, 3067−3078. (b) Cheng, L.; Coville, N. J. *J. Organomet. Chem.* **1998**, *556*, 111−118. (c) Bogadi, R. S.; Levendis, D. C.; Coville, N. J. *J. Am. Chem. Soc.* **2002**, *124*, 1104−1110. (d) Katsuki, K.; Ooyama, Y.; Okamoto, M.; Yamamoto, Y. *Inorg. Chim. Acta* **1994**, *217*, 181−185.

(23) (a) Lavigne, G.; Lugan, N.; Rivomanana, S.; Mulla, F.; Soulié, J.-M.; Kalck, P. *J. Cluster Sci.* **1993**, *4*, 49−58. (b) Cabeza, J. A.; Fernández-Colinas, J. M. *Coord. Chem. Rev.* **1993**, *126*, 319−336.

(24) (a) Tebbe, F. N.; Meakin, P.; Jesson, J. P.; Muetterties, E. L. *J. Am. Chem. Soc.* **1970**, *92*, 1068−1070. (b) Darensbourg, D. J.; Baldwin, B. J. *J. Am. Chem. Soc.* **1979**, *92*, 6447−6449. (c) Springer, C. S., Jr.; Sievers, R. E. *Inorg. Chem.* **1967**, *6*, 852−854. (d) Muetterties, E. L. *J. Am. Chem. Soc.* **1968**, *90*, 5097−5102.

(25) Howell, J. A. S.; Burkinshaw, P. M. *Chem. Rev.* **1983**, *83*, 557−599.

(26) (a) Purcell, K. F. *J. Am. Chem. Soc.* **1979**, *101*, 5147−5152. (b) Darensbourg, D. J.; Gray, R. L. *Inorg. Chem.* **1984**, *23*, 2993−2996. (c) Darensbourg, D. J. *Inorg. Chem.* **1979**, *18*, 14−17.

(27) Ismail, A. A.; Sauriol, F.; Butler, I. S. *Inorg. Chem.* **1989**, *28*, 1007−1012.

(28) (a) Darensbourg, D. J.; Darensbourg, M. Y.; Gray, R. L.; Simmons, D.; Arndt, L. W. *Inorg. Chem.* **1986**, *25*, 880−882. (b) Soubra, C.; Oishi, Y.; Albright, T. A.; Fujimoto, H. *Inorg. Chem.* **2001**, *40*, 620−627.

(29) Theoretical relative stability in *meso*-free derivatives (**2a′−c′**) is different from that in *meso*-phenyl derivatives (**2a−c**).